Journal of the American College of Cardiology
© 2004 by the American College of Cardiology Foundation
Published by Elsevier Inc.

Vol. 44, No. 7, 2004
ISSN 0735-1097/04/$30.00
doi:10.1016/j.jacc.2004.06.067

Tissue Doppler-Derived Myocardial Acceleration for Evaluation of Left Ventricular Diastolic Function

Ikuo Hashimoto, MD,* Aarti Hejmadi Bhat, MD,* Xiaokui Li, MD,* Michael Jones, MD,† Crispin H. Davies, MD,* Julia C. Swanson, BS,* Sebastian T. Schindera, MD,* David J. Sahn, MD, MACC*

Portland, Oregon; and Bethesda, Maryland

OBJECTIVES Our purpose was to evaluate a tissue Doppler-based index—peak myocardial acceleration (pACC)—during isovolumic relaxation and in evaluating left ventricular (LV) diastolic function.

BACKGROUND Simple, practical indexes for diastolic function evaluation are lacking, but are much desired for clinical evaluation.

METHODS We examined eight sheep by using tissue Doppler ultrasound images obtained in the apical four-chamber views to evaluate mitral valve annular velocity at the septum and LV wall. The pACC thus derived was analyzed during isovolumic relaxation (IVRT) and during the LV filling period (LVFP). We then changed the hemodynamic status of each animal by blood administration, dobutamine, and metoprolol infusion. We compared the pACC values during IVRT and LVFP over the four different hemodynamic conditions with a peak rate of drop in LV pressure ($-dP/dt_{min}$) and the time constant of LV isovolumic pressure decay (tau), as measured with a high-frequency manometer-tipped catheter.

RESULTS The pACC of the septal side of the mitral valve annulus during IVRT showed a good correlation with $-dP/dt_{min}$ ($r = -0.80$, $p < 0.0001$) and tau ($r = -0.87$, $p < 0.0001$). The mean left atrial pressure (LAP) correlated well with the septal side pACC during LVFP ($r = 0.81$, $p < 0.0001$). There was a weak correlation between the mitral valve annulus pACC at the LV lateral wall and mean LAP.

CONCLUSIONS The pACC during IVRT is a sensitive, preload-independent marker for evaluation of LV diastolic function. In addition, pACC during LVFP correlated well with mean LAP. (J Am Coll Cardiol 2004;44:1459–66) © 2004 by the American College of Cardiology Foundation

Evaluation and recognition of left ventricular (LV) diastolic dysfunction is important for managing patients with serious heart failure (1). Unlike systolic dysfunction, a simple method for evaluating diastolic dysfunction is elusive, and most methods are difficult to understand because not only myocardial compliance but also several other factors, such as heart rate, LV diastolic suction, left atrial pressure (LAP), and left atrial contraction, among others, are related to ventricular diastolic function (2,3).

Tissue Doppler imaging (TDI) has been reported to be a powerful modality that enables assessment of ventricular wall motion with a high temporal and spatial resolution (4–7). Measurement of mitral annulus displacement along the LV long axis has been proposed as a method for assessment of LV systolic and diastolic function (8–10). The early diastolic mitral valve annular velocity (E_a) observed by TDI is related to LV diastolic function and tends to decrease with impaired myocardial relaxation (8,9,11,12). On the other hand, it is well known that the elevation of LV filling pressure accelerates the velocity of transmitral early rapid filling (E) (8,13). Therefore, several investigators have already reported that E/E_a has a strong correlation with LV filling pressure (3,13,14). Noninvasive estimation of filling pressure is also important for management of patients with heart failure. However, E and E_a waves need to be measured separately, and so the measurement is cumbersome.

Recently, ultrasound-derived myocardial acceleration (ACC) during isovolumic contraction has been reported to be a good index for evaluation of ventricular function (15). We and others (15,16) have shown that peak ACC (pACC) during systole was related to myocardial contractility, especially for the period of acceleration during isovolumic contraction. Although the forces affecting pACC must be more complex during diastole, the peak acceleration during the isovolumic relaxation time (IVRT) could relate to active or passive release of torsion, and the peak acceleration during diastolic filling could be related to LV filling pressure.

The purpose of our present study was to assess the feasibility of using both of these pACC measurements for evaluating LV diastolic function in an animal model.

METHODS

Experimental preparation. Eight sheep (weight 35 to 47 kg [mean 40.1 ± 4.2 kg]) were studied. All sheep underwent thoracotomy under general anesthesia induced with intravenous sodium pentobarbital (25 mg/kg body weight) and maintained by using 1% to 2% isoflurane with oxygen. The sheep were intubated and ventilated with a volume-

From the *Clinical Care Center for Congenital Heart Disease, Oregon Health and Science University, Portland, Oregon; and †National Heart, Lung, and Blood Institute, Bethesda, Maryland. Dr. Sahn is an occasional consultant to GE Medical Systems, but this relationship has had no effect on this study.

Manuscript received December 1, 2003; revised manuscript received June 23, 2004, accepted June 29, 2004.

Abbreviations and Acronyms

ACC = myocardial acceleration
IVRT = isovolumic relaxation time
IVS = interventricular septum
LAP = left atrial pressure
LV = left ventricle/ventricular
LVFP = left ventricular filling period
pACC = peak myocardial acceleration
tau = time constant of LV isovolumic pressure decay
TDI = tissue Doppler imaging

cycle respirator. An electrocardiogram was monitored from a limb lead. Intracavity manometer-tipped catheters (model SPC-350, Millar Instruments, Inc., Houston, Texas) were placed in the LV through a carotid artery and in the left atrium via the appendage, respectively, for pressure recording. Peak rate of drop in LV pressure ($-dP/dt_{min}$) was obtained from the first derivative of pressure curve of the LV. The time constant of LV isovolumic pressure decay (tau) was also measured according to the method proposed by Weiss et al. (17). Both $-dP/dt_{min}$ and tau were used for the evaluation of global diastolic function (18–21). Another catheter was positioned in the femoral artery to monitor systemic arterial pressure and blood gas. These catheters were interfaced with a physiologic recorder (ES 2000, Gould Medical Products Division, Oxnard, California) with a fluid-filled pressure transducer (model PD231D, Gould Medical Products Division). Two electromagnetic flow probes (model EP455, Carolina Medical, Inc., King, North Carolina) were placed: one around the skeletonized ascending aorta distal to the coronary ostia and proximal to the bronchiocephalic trunk and the second around the pulmonary artery just above the pulmonary valve to measure cardiac output. Both flow probes were connected to flow meters (model FM501, Carolina Medical Electronics) and interfaced to the same physiologic recorder (ES 2000, Gould) that was used for pressure recording. All hemodynamic data were recorded at a paper speed of 250 mm/s. Four consecutive cardiac cycles were analyzed for each hemodynamic determination. All operative and animal management procedures were approved by the Animal Care and Use Committee of the National Heart, Lung, and Blood Institute, National Institutes of Health, Bethesda, Maryland.

Experimental protocol. Baseline, volume loading, and dobutamine and metoprolol infusion were used to produce a total of four different hemodynamic conditions for each animal. After a baseline recording, 500 ml blood was infused slowly, then intravenous dobutamine (2 to 10 μg/kg/min) and 5 mg metoprolol were administered at least 1 h after the previous stage. All of the hemodynamic and myocardial velocity data (described subsequently) were acquired simultaneously at each hemodynamic stage with transient suspension of ventilation for the short period of data acquisition.

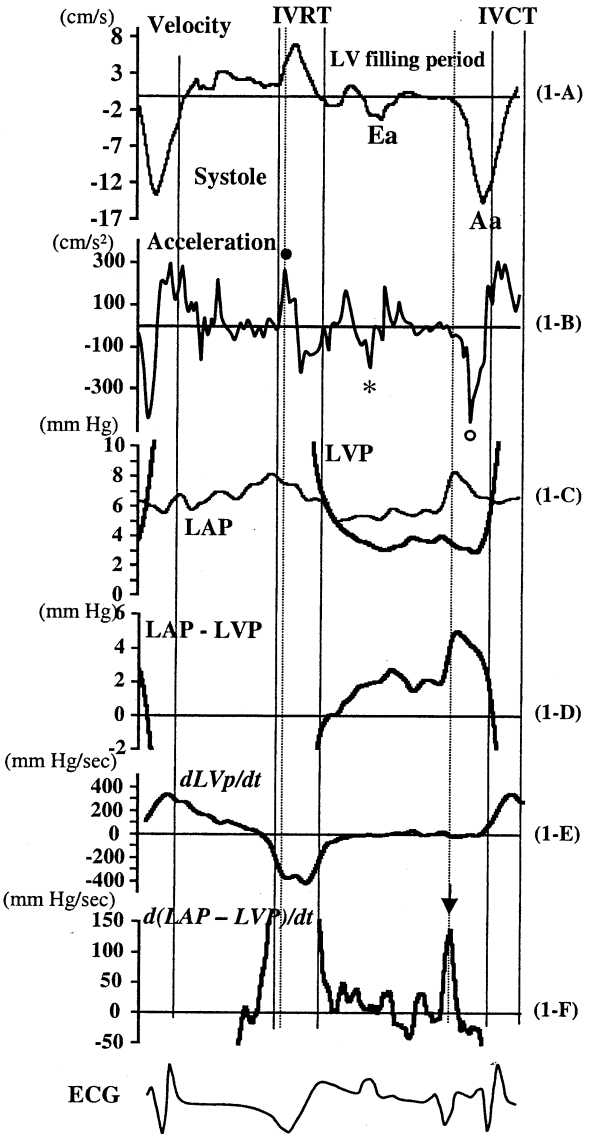

Figure 1. Representative tissue velocity and myocardial acceleration of the septal mitral valve annulus and synchronized waveforms of LV pressure (LVP) and left atrial pressure (LAP). Early diastolic annular velocity (E_a) and late diastolic annular velocity (A_a) were noted in velocity curve **1-A**. Definite positive peaks for myocardial acceleration were noted during isovolumic relaxation time (IVRT) **(•)**, and a negative peak for acceleration at the beginning of the left ventricular filling period **(*)** was also noted corresponding to the E_a wave in ACC curve **1-B**. The LVP and LAP were displayed together **(1-C)**, and the difference between LAP and LVP was shown in **1-D**. The derivative of LV pressure (dLVp/dt) was also displayed in **1-E**. The derivative of the difference between LAP and LVP was calculated and displayed in **1-F**. ECG = electrocardiogram.

Echocardiographic analysis. We used a Vivid FiVe digital ultrasound system (GE/VingMed Ultrasound, Horten, Norway) for this study. Scanning was performed longitudinally from the apex to acquire an apical four-chamber view with a 5.0-MHz phased-array transducer. The TDI sector angle was limited to that required to encompass the LV cavity and walls, and the line density and packet size were adjusted for smooth, consistent data with the maximized frame rate. The TDI data

Table 1. Hemodynamic Parameters in Each Condition

	Baseline	Blood Loading	Dobutamine	Metoprolol
Cardiac output (l/min)	1.62 ± 0.47	2.2 ± 0.48*	2.0 ± 0.48	1.54 ± 0.24
Heart rate (beats/min)	100 ± 12	106 ± 6	142 ± 25*	81 ± 8*
LVEDP (mm Hg)	12.1 ± 4.2	16.2 ± 6.2	11.1 ± 5.9	15.3 ± 2.1
Mean LAP (mm Hg)	9.9 ± 2.9	13.8 ± 2.9†	9.1 ± 2.8*	10.7 ± 2.3
$-dP/dt_{min}$ (mm Hg/s)	−1,083 ± 183	−1,290 ± 137*	−1,391 ± 295*	−667 ± 277*
Tau (ms)	47.5 ± 6.1	44.0 ± 7.5	40.0 ± 9.6*	56.2 ± 4.5*

*$p < 0.05$ compared with baseline. †$p < 0.005$ compared with baseline. Data are presented as the mean value ± SD.
LAP = left atrial pressure; LVEDP = left ventricular end-diastolic pressure; tau = time constant for left ventricular relaxation.

of septal and lateral mitral valve annulus were acquired with a pulse repetition frequency from 1.0 to 4.5 kHz and a frame rate varying from 80 to 130 frames/s, as maximized as possible. To retain the same sampling region, an autotracking technique was used for all measurements. Setting of autotracking for each sampling point was carefully performed so as not to deviate from the wall zone.

Autotracking is a newly developed modality that allows semiautomatic correction of sampling position, tracking specific tissue speckles throughout the heart cycle. With these settings, no aliasing of velocities was encountered. The TDI data for the two-dimensional images for two to three cycles for each stage were stored on magnetic optical disk, with subsequent off-line analysis of scan-line digital data. Optimized TDI data for the two-dimensional images of the heart for each stage were analyzed using the EchoPac 6.3 (archiving application software of Vivid FiVe). This software allowed us to evaluate several different locations of tissue velocity simultaneously and display velocity-time relationship curves for each.

After obtaining frame-by-frame velocity values, myocardial velocity acceleration was calculated as the difference between two sequential velocities divided by frame-by-frame time interval. The interval for calculation was consistently set from 20 to 25 ms, averaging consecutive two to three velocity determinations. Acceleration curves were obtained from each calculation (Fig. 1). Acceleration curves showed positive peaks during IVRT and a negative peak corresponding to E_a. The IVRT was also determined by opening the mitral valve on the simultaneous cine loop. We measured pACC during IVRT and LV filling period (LVFP) and compared these values with mean LAP or pressure-derived peak dP/dt in the present study.

Interobserver variability. The interobserver variability was tested in 10 randomly selected datasets from four sheep measured at different times from digital recordings by two separate observers, each without knowledge of the other's measurement.

Statistics. All data are expressed as the mean value ± SD. One-way repeat measures analysis of variance was performed to compare ACC between four different hemodynamic conditions, and Dunnett's method was used for the post-hoc test. Linear regression analysis was used for comparison between peak ACC and mean LAP and peak dP/dt as a hemodynamic parameter. All statistical analyses were performed using StatView version 5.01 (SAS Institute, Cary, North Carolina). A p value <0.05 was regarded as significant.

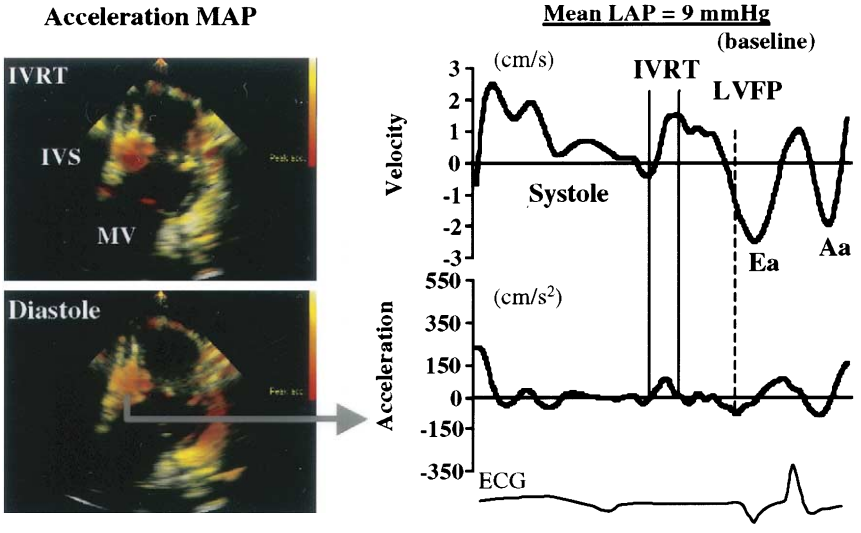

Figure 2. Two-dimensional myocardial acceleration map during IVRT **(upper left)** and during LVFP **(lower left)**. The tissue velocity and ACC waveform for IVS are shown **(right)** in the baseline condition (LAP of 9 mm Hg). MAP = mean atrial pressure; MV = mitral valve; other abbreviations as in Figure 1.

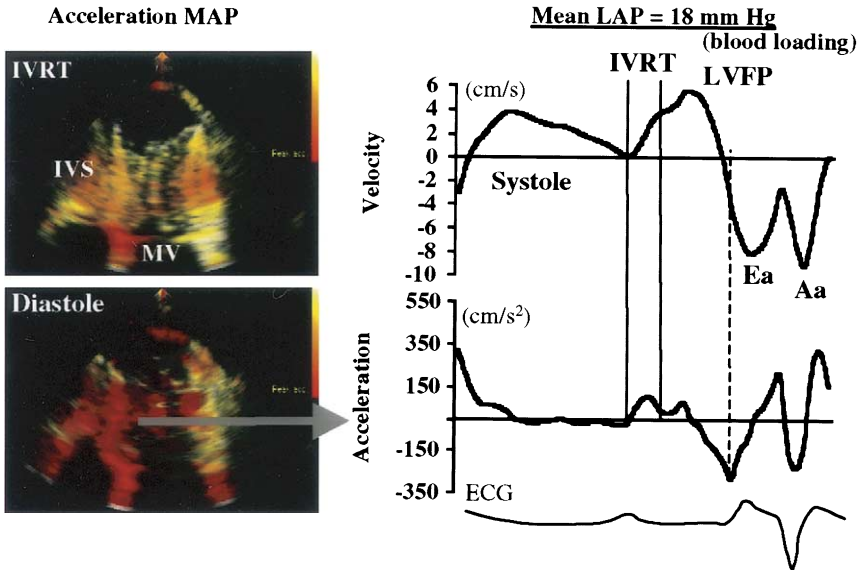

Figure 3. A myocardial acceleration map during IVRT **(left upper column)** and during LVFP **(left lower column)** in blood loading (LAP of 18 mm Hg). Abbreviations as in Figures 1 and 2.

RESULTS

Change in hemodynamics during study. Table 1 shows the hemodynamics related to each stage. From baseline, cardiac output significantly increased from 1.62 ± 0.47 l/min to 2.2 ± 0.48 l/min by blood loading and to 2.0 ± 0.48 l/min by dobutamine infusion. The heart rate also significantly changed from 100 ± 12 beats/min to 142 ± 25 beats/min by dobutamine infusion. Left ventricular end-diastolic pressure did not show a statistically significant change between stages. However, LAP significantly increased from 9.9 ± 2.9 mm Hg to 13.8 ± 2.9 mm Hg by blood loading ($p < 0.005$) and decreased to 9.1 ± 2.8 mm Hg by dobutamine infusion ($p < 0.05$). The $-dP/dt_{min}$ also significantly changed in each hemodynamic condition ($p < 0.05$). Metoprolol significantly decreased $-dP/dt_{min}$ compared with baseline ($p < 0.05$), but the LAP change with metoprolol was not significant. Tau showed a significant change with dobutamine and metoprolol infusion ($p < 0.05$).

Relation of ACC curves to hemodynamics. Figure 1 shows a representative tissue velocity for the septal side of the mitral valve annulus (1-A) and ACC curves (1-B) in the baseline condition. Synchronized waveforms of LV and atrial pressure (LVP and LAP, 1-C), the difference between LAP and LVP (LAP − LVP, 1-D), derivative of LVP (1-E), and derivative of (LAP − LVP) (1-F) are displayed. In velocity curve 1-A, distinctive E_a and early diastolic annular velocity (A_a) waves are noted during LVFP. The ACC curve 1-B showed a definite positive peak wave (closed circle) during IVRT and subsequent negative peak wave (*) corresponding to the E_a wave during LVFP. The pressure difference between LAP and LVP (1-D) showed two peaks corresponding to E_a and A_a during LVFP. The derivative curve from LAP − LVP (Fig. 1, 1-F), atrial contraction yielded a definite sharp peak (closed arrow), and this peak preceded acceleration of the A_a wave (open circle).

Correlation between pACC and mean LAP. Figure 2 shows an ACC map of the interventricular septum (IVS)

Table 2. Correlation Coefficients (r) Between Each Variable and LAP, $-dP/dt_{min}$, or Tau

Variables	Mean ± SD	LAP	$-dP/dt_{min}$	Tau
E, septal (cm/s)	3.9 ± 2.1	0.43	−0.58†	−0.71†
E, lateral (cm/s)	4.3 ± 1.9	0.29	−0.19	−0.22
A, septal (cm/s)	7.4 ± 3.0	0.19	−0.62†	−0.48*
A, lateral (cm/s)	6.8 ± 3.7	0.15	−0.54*	−0.50*
E/A ratio, septal	0.99 ± 0.82	0.33	−0.08	0.04
E/A ratio, lateral	0.64 ± 0.28	0.08	0.48	0.24
pACC during IVRT, septal (cm/s^2)	104.8 ± 49.6	0.18	−0.80‡	−0.87‡
pACC during IVRT, lateral (cm/s^2)	83.4 ± 40.6	0.17	−0.54*	−0.67†
pACC during LVFP, septal (cm/s^2)	131.5 ± 62.5	0.81‡	0.30	0.36
pACC during LVFP, lateral (cm/s^2)	116.2 ± 54.8	0.52*	0.10	0.29

*$p < 0.05$. †$p < 0.005$. ‡$p < 0.0001$.
IVRT = isovolumic relaxation time; LVFP = left ventricular filling period; pACC = peak myocardial acceleration; other abbreviations as in Table 1.

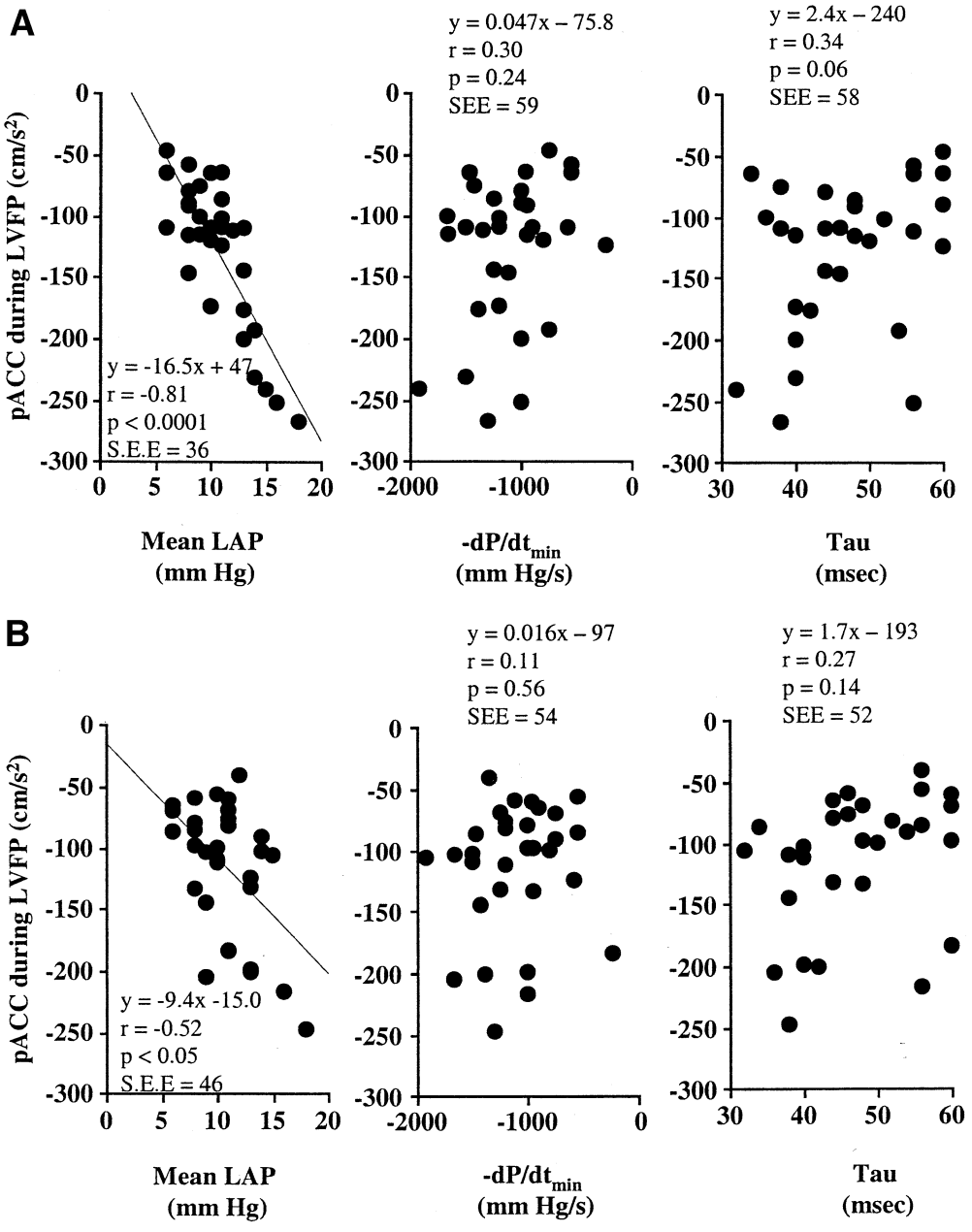

Figure 4. Relationship of septal peak myocardial acceleration (pACC) **(A)** and left ventricular lateral pACC **(B)** during LVFP to mean LAP **(left)**, $-dP/dt_{min}$ **(middle)**, and tau **(right)** in all experimental stages (n = 32). Abbreviations as in Figure 1.

during IVRT (left upper column) and during LVFP (left lower column), as well as tissue velocity and ACC waveform (right column) in the baseline condition (LAP of 9 mm Hg). The ACC was calculated from tissue velocity and displayed as a red gradient superimposed on the myocardial image. During IVRT, the IVS was coded with red, but the LV free wall was not stained as much. During LVFP, both the IVS and free wall were coded red. Septal pACC showed 69.5 cm/s^2 during IVRT and 79.2 cm/s^2 during LVFP. On the other hand, IVS displayed a red code after blood loading during LVFP (LAP of 18 mm Hg) (Fig. 3). The acceleration curve also showed increasing negative peak during LVFP (252.3 cm/s^2). However, the ACC curve did not show a significant change during the IVRT (97.7 cm/s^2).

Table 2 shows the correlation between LAP, pressure-derived $-dP/dt_{min}$, or tau and other variables. Only peak ACC during LVFP showed a significant correlation between LAP (septum: $r = -0.81$, $p < 0.0001$, lateral wall: $r = -0.52$, $p < 0.05$) (Figs. 4A and 4B). In contrast, the pACC of IVS during IVRT showed a strong correlation with peak negative dP/dt ($r = -0.80$, $p < 0.0001$) and tau ($r = -0.87$, $p < 0.0001$) (Figs. 5A and 5B). However, the pACC during LVFP did not correlate with either $-dP/$

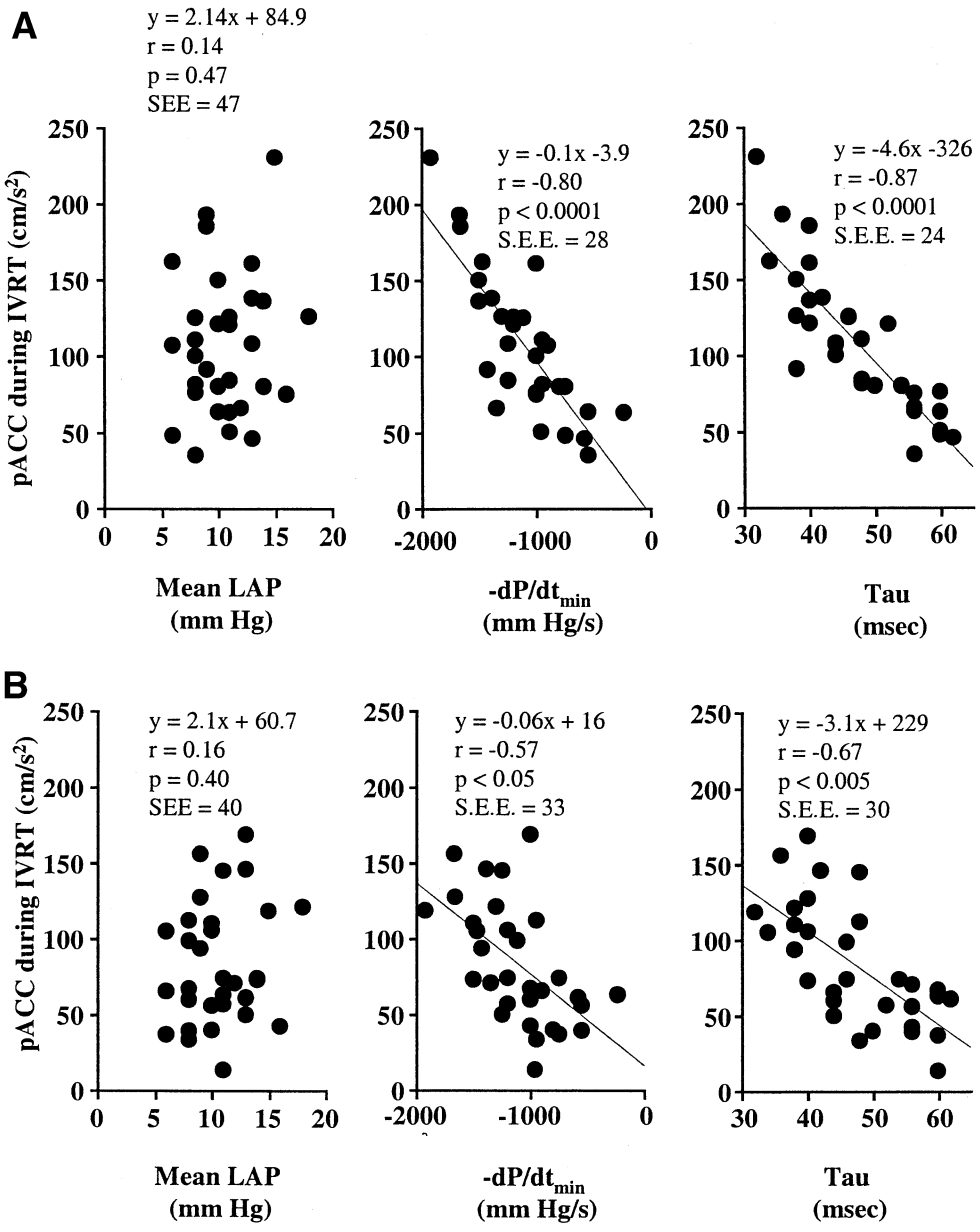

Figure 5. Relationship of septal pACC **(A)** and LV lateral pACC **(B)** during IVRT to mean LAP **(left)**, $-dP/dt_{min}$ **(middle)**, and tau **(right)** in all experimental stage (n = 32). Abbreviations as in Figures 1 and 4.

dt_{min} or tau. Therefore, mean LAP significantly correlated with peak ACC during LVFP but did not correlate with pACC during IVRT in either the IVS or lateral wall.

Table 3 shows the alteration of TDI variables with hemodynamic changes. Septal ACC during LVFP was significantly increased from 117 ± 43.5 cm/s to 209.1 ± 47.3 cm/s by blood loading ($p < 0.05$). Lateral pACC also increased by blood loading, but the change was not statistically significant. Neither dobutamine nor metoprolol significantly changed pACC during LVFP. The pACC during IVRT changed in response to each hemodynamic condition, but the changes were not statistically significant. The E wave of the septum was changed significantly by blood loading and dobutamine infusion (blood loading: $p < 0.05$; dobutamine infusion: $p < 0.05$). The pACC of the IVS was significantly larger than that of the LV wall both during IVRT ($p < 0.005$) and LVFP ($p < 0.05$).

Interobserver variability. The linear regression between two observers (Drs. Hashimoto and Li) for the measurement of pACC showed very good reproducibility for IVRT ($r = 0.97$, $p < 0.0001$) as well as for LVFP ($r = 0.96$, $p < 0.0001$).

DISCUSSION

This is the first investigation to examine the feasibility and utility of using TDI velocity-derived myocardial acceleration determination for the evaluation of LV diastolic function. Tissue Doppler acceleration imaging is a new measurement

Table 3. Alteration of Each Variable With Hemodynamic Changes

	Baseline	Blood Loading	Dobutamine	Metoprolol
E, septal (cm/s)	3.2 ± 1.8	5.8 ± 2.0*	6.3 ± 3.2*	2.1 ± 1.1
E, lateral (cm/s)	3.1 ± 1.1	5.4 ± 2.3*	4.1 ± 1.7	3.8 ± 1.7
A, septal (cm/s)	6.6 ± 2.9	8.4 ± 2.4	9.3 ± 2.5*	3.8 ± 1.8*
A, lateral (cm/s)	5.0 ± 2.9	8.4 ± 2.4	11.0 ± 4.7†	3.5 ± 2.2
E/A ratio, septal	0.57 ± 0.23	0.86 ± 0.15	0.59 ± 0.31	0.84 ± 0.31
E/A ratio, lateral	0.74 ± 0.56	1.0 ± 0.6*	0.53 ± 0.35	1.54 ± 1.16*
pACC during IVRT, septal (cm/s^2)	109.9 ± 33.2	106.2 ± 30.9	143.1 ± 65.6	70.2 ± 29.8
pACC during IVRT, lateral (cm/s^2)	87.0 ± 47.3	93.2 ± 38.0	100.1 ± 40.6	59.9 ± 30.3
pACC during LVFP, septal (cm/s^2)	117 ± 43.5	209.1 ± 47.3*	118.9 ± 63.3	100.9 ± 47.8
pACC during LVFP, lateral (cm/s^2)	94.4 ± 48.0	153.6 ± 80.2	125.6 ± 40.5	100.1 ± 43.6

*$p < 0.05$ compared with baseline. †$p < 0.005$ compared with baseline. Data are presented as the mean value ± SD. Abbreviations as in Table 2.

based on TDI and obtained from a derivative of tissue velocity. High temporal and spatial resolution makes it possible to display and detect intramural abnormal rhythm conduction in the heart, and acceleration mapping has been used for detection of the pre-excitation region in patients with Wolff-Parkinson-White syndrome (22,23). However, the feasibility of studying myocardial acceleration has not been studied as a use for evaluating ventricular diastolic function. Myocardial acceleration and the rate of change of ventricular cavity pressure (dP/dt), which have been used as indexes of contractility or relaxation, show parallel alterations, because intracavity pressure change is caused by myocardial contraction or relaxation, especially during isovolumic periods. Vogel et al. (15) reported that myocardial acceleration during isovolumic contraction time was a good index for evaluation of right ventricular contraction and was less preload and afterload dependent than other indexes.

The behavior of pACC was different, however, during IVRT and LVFP, as shown in our data. The pACC during septal IVRT correlated with both pressure-derived $-dP/dt_{min}$ and tau but did not correlate with mean LAP. In contrast, pACC during LVFP correlated with mean LAP but did not correlate with either $-dP/dt_{min}$ or tau. We observed that peak d(LAP − LVP)/dt induced by atrial contraction preceded the pACC caused by atrial myocardial contraction. The pressure gradient between LV and LA during the filling period therefore affects LV wall motion and may be correlated with myocardial acceleration during the filling period.

Estimation of mean LAP. A number of methods have been developed for estimation of mean LAP. Several studies have reported that conventional mitral flow had a weak correlation with LAP, but related better to LAP when corrected for the influence of LV relaxation (3,11,13,14). The E_a wave of the mitral valve annulus and flow propagation velocity are relatively less preload dependent and are good indexes of LV relaxation and used for correction of the E wave (E/E_a) (11). Ommen et al. (3) reported that there remained significant scatter with E/E_a for estimation of LAP, particularly with intermediate values of E/E_a. Nagueh et al. (24) reported that E_a correlated well with the maximal transmitral pressure gradient, but lost influence of filling pressure once LV relaxation was impaired. The pACC may be related to LV relaxation or elastic recoil and could be increased when responding to preload elevation, as long as LV relaxation was maintained. However, the relationship between pACC and preload when metoprolol was administrated was not examined as effectively in the present study because LAP did not change significantly. To get the wider range of LAP values, we probably would have needed to administer more blood volume than 500 ml.

Difference of ACC between IVS and LV lateral wall. There was a significant difference in the pACC patterns between the IVS and LV lateral wall. The pACC values for the IVS were consistently larger than those for the LV lateral wall in the present study. Also, the pACC of the IVS correlated well with hemodynamic data on mean LAP, pressure-derived $-dP/dt_{min}$, and tau. However, the correlation between the pACC of the LV lateral wall and these same hemodynamic data was weaker. Ommen et al. (3) also indicated that measurement of the medial annulus was more sensitive and demonstrated a better correlation with LV filling pressure than did measurement of the lateral annulus. As Rodriguez et al. (8) described, the mitral annular ring motion has a complex three-dimensional pattern with longitudinal, rotational, and sphincter-like motion. However, Donofrio et al. (25) analyzed regional wall motion using three-dimensional magnetic resonance imaging and found that heterogeneity of septal strain was less than that of other LV wall segments. Moore et al. (26) also described that radial and circumferential IVS displacements were smaller than those of other LV wall segments. From the histologic point of view, the IVS is formed by three muscle strata. The middle and left-sided layers, which consist of the fibers of the ascending and descending bundles, respectively, may play a more important role in longitudinal ventricular contraction and relaxation (27). The basal loop of the right and left segments, which correspond to the LV or RV lateral wall, contribute to circumferential narrowing or widening of ventricle and would be less well characterized by the method and views we used. Further anatomic knowledge about these

aspects of cardiac anatomy and physiology may also clarify our findings in the future.

The sampling rate is an important scanning parameter for this technique. The sampling rate we used for this study was from 80 to 130 frames/s. The sampling interval became 7.6 to 12.5 ms. The normal IVRT is about 40 to 50 ms. In this setting, we could get three to five sampling points during IVRT. Ideally, more than five points would be desirable for calculation of acceleration. However, with an increasing sampling rate, we cannot ignore the influence of random noise contained in TDI sampling data. A high sampling rate may augment noise on the acceleration curve. To cancel out this random noise, TDI sampling data can be averaged over two to three beats. However, averaging of serial beats may broaden peaks and troughs. The sampling rate required to accurately make these measurement depends on image quality, the range of values, and the processing method and has not yet been definitively established.

Conclusions. In our study, we showed that the pACC of the septum correlated with $-dP/dt_{min}$, as well as tau, during IVRT, indicating the dominant role of LV relaxation or passive recoil in this cardiac phase. During LVFP, the pACC of the septum correlated much better with the mean LAP than $-dP/dt_{min}$ or tau, indicating that the pressure gradient between LA and LV and atrial contraction are dominant factors during this period. The septal wall seems to reflect these parameters much more closely than the lateral wall. Use of those indexes, especially for determining measurements of septal acceleration, may simplify the approach to evaluation of diastolic function.

Reprint requests and correspondence: Dr. David J. Sahn, L608, Pediatric Cardiology, Oregon Health and Science University, 3181 S.W. Sam Jackson Park Road, Portland, Oregon 97239-3098. E-mail: sahnd@ohsu.edu.

REFERENCES

1. Zile MR, Gaasch WH, Carroll JD, et al. Heart failure with a normal ejection fraction: is measurement of diastolic function necessary to make the diagnosis of diastolic heart failure? Circulation 2001;104: 779–82.
2. Nishimura RA, Tajik AJ. Evaluation of diastolic filling of left ventricle in health and disease: Doppler echocardiography is the clinician's Rosetta stone. J Am Coll Cardiol 1997;30:8–18.
3. Ommen SR, Nishimura RA, Appleton CP, et al. Clinical utility of Doppler echocardiography and tissue Doppler imaging in the estimation of left ventricular filling pressures: a comparative simultaneous Doppler-catheterization study. Circulation 2000;102:1788–94.
4. Nagueh SF, Bachinski LL, Meyer D, et al. Tissue Doppler imaging consistently detects myocardial abnormalities in patients with hypertrophic cardiomyopathy and provides a novel means for an early diagnosis before and independently of hypertrophy. Circulation 2001; 104:128–30.
5. Harada K, Tsuda A, Orino T, Tanaka T, Takada G. Tissue Doppler imaging in the normal fetus. Int J Cardiol 1999;71:227–34.
6. Miyatake K, Yamagishi M, Tanaka N, et al. New method for evaluating left ventricular wall motion by color-coded tissue Doppler imaging: in vitro and in vivo studies. J Am Coll Cardiol 1995;25:717–24.
7. Oki T, Iuchi A, Tabata T, et al. Left ventricular systolic wall motion velocities along the long and short axes measured by pulsed tissue Doppler imaging in patients with atrial fibrillation. J Am Soc Echocardiogr 1999;12:121–8.
8. Rodriguez L, Garcia M, Ares M, Griffin BP, Nakatani S, Thomas JD. Assessment of mitral annular dynamics during diastole by Doppler tissue imaging: comparison with mitral Doppler inflow in subjects without heart disease and in patients with left ventricular hypertrophy. Am Heart J 1996;131:982–7.
9. Sohn DW, Chai IH, Lee DJ, et al. Assessment of mitral annulus velocity by Doppler tissue imaging in the evaluation of left ventricular diastolic function. J Am Coll Cardiol 1997;30:474–80.
10. Garcia MJ, Rodriguez L, Ares M, Griffin BP, Thomas JD, Klein AL. Differentiation of constrictive pericarditis from restrictive cardiomyopathy: assessment of left ventricular diastolic velocities in longitudinal axis by Doppler tissue imaging. J Am Coll Cardiol 1996;27:108–14.
11. Gonzalez-Vilchez F, Ares M, Ayuela J, Alonso L. Combined use of pulsed and color M-mode Doppler echocardiography for the estimation of pulmonary capillary wedge pressure: an empirical approach based on an analytical relation. J Am Coll Cardiol 1999;34:515–23.
12. Nagueh SF, Mikati I, Kopelen HA, Middleton KJ, Quinones MA, Zoghbi WA. Doppler estimation of left ventricular filling pressure in sinus tachycardia: a new application of tissue Doppler imaging. Circulation 1998;98:1644–50.
13. Harada K, Tamura M, Yasuoka K, Toyono M. A comparison of tissue Doppler imaging and velocities of transmitral flow in children with elevated left ventricular preload. Cardiol Young 2001;11:261–8.
14. Nagueh SF, Lakkis NM, Middleton KJ, Spencer WH 3rd, Zoghbi WA, Quinones MA. Doppler estimation of left ventricular filling pressures in patients with hypertrophic cardiomyopathy. Circulation 1999;99:254–61.
15. Vogel M, Schmidt MR, Kristiansen SB, et al. Validation of myocardial acceleration during isovolumic contraction as a novel noninvasive index of right ventricular contractility: comparison with ventricular pressure-volume relations in an animal model. Circulation 2002;105:1693–9.
16. Vogel M, Cheung MM, Li J, et al. Noninvasive assessment of left ventricular force-frequency relationships using tissue Doppler-derived isovolumic acceleration: validation in an animal model. Circulation 2003;107:1647–52.
17. Weiss JL, Frederiksen JW, Weisfeldt ML. Hemodynamic determinants of the time-course of fall in canine left ventricular pressure. J Clin Invest 1976;58:751–60.
18. Greenberg NL, Firstenberg MS, Castro PL, et al. Doppler-derived myocardial systolic strain rate is a strong index of left ventricular contractility. Circulation 2002;105:99–105.
19. Jamal F, Strotmann J, Weidemann F, et al. Noninvasive quantification of the contractile reserve of stunned myocardium by ultrasonic strain rate and strain. Circulation 2001;104:1059–65.
20. Saito A, Shiono M, Orime Y, et al. Effects of left ventricular assist device on cardiac function: experimental study of relationship between pump flow and left ventricular diastolic function. Artif Organs 2001;25:728–32.
21. Miyashita T, Okano Y, Takaki H, Satoh T, Kobayashi Y, Goto Y. Relation between exercise capacity and left ventricular systolic versus diastolic function during exercise in patients after myocardial infarction. Coron Artery Dis 2001;12:217–25.
22. Eder V, Marchal C, Tranquart F, Sirinelli A, Pottier JM, Cosnay P. Localization of the ventricular preexcitation site in Wolff-Parkinson-White syndrome with Doppler tissue imaging. J Am Soc Echocardiogr 2000;13:995–1001.
23. Yin LX, Li CM, Fu QG, et al. Ventricular excitation maps using tissue Doppler acceleration imaging: potential clinical application. J Am Coll Cardiol 1999;33:782–7.
24. Nagueh SF, Sun H, Kopelen HA, Middleton KJ, Khoury DS. Hemodynamic determinants of the mitral annulus diastolic velocities by tissue Doppler. J Am Coll Cardiol 2001;37:278–85.
25. Donofrio MT, Clark BJ, Ramaciotti C, et al. Regional wall motion and strain of transplanted hearts in pediatric patients using magnetic resonance tagging. Am J Physiol 1999;277:R1481–7.
26. Moore CC, Lugo-Olivieri CH, McVeigh ER, Zerhouni EA. Three-dimensional systolic strain patterns in the normal human left ventricle: characterization with tagged MR imaging. Radiology 2000;214:453–466.
27. Torrent-Guasp F, Buckberg GD, Clemente C, Cox JL, Coghlan HC, Gharib M. The structure and function of the helical heart and its buttress wrapping. I. The normal macroscopic structure of the heart. Semin Thorac Cardiovasc Surg 2001;13:301–19.